10

The creation of a quarter-wave phase plate in bulk of fused silica by the femtosecond laser writing

© P.A. Danilov[1,2], G.K. Krasin[1], A.E. Rupasov[1], A.V. Gorevoy[1], M.S. Kovalev[1,2], I.N. Mushkarina[1,2], A.S. Komshin[2], S.I. Kudryashov[1,2]

[1] Lebedev Physical Institute, Russian Academy of Sciences, Moscow, Russia
[2] Bauman Moscow State Technical University, Moscow, Russia

e-mail: danilovpa@lebedev.ru

Received October 22, 2025
Revised December 12, 2025
Accepted February 21, 2026

Using the method of direct laser writing with femtosecond pulses, a three-dimensional micro-optical element has been formed in bulk of a fused silica plate, functioning as a quarter-wave phase plate at a wavelength of 633 nm. It has been shown that the induced birefringence ($\Delta n \approx 3 \cdot 10^{-4}$) is due to the formation of an anisotropic type II modification, accompanied by the generation of oxygen-deficient and nonbridging oxygen hole defect centers. Photoluminescence and Raman scattering spectroscopy confirmed a uniform distribution of defects throughout the modified area and a local reorganization of the amorphous SiO_2 matrix. High transmission (60−80%) in the range of 600−1100 nm and strong UV absorption due to defects were established. It was demonstrated that the position of the area of maximum modification is shifted relative to the geometric focal plane due to the nonlinear self-focusing effect, which was confirmed by a quantitative assessment of the nonlinear focus position. The obtained results demonstrate the potential for creating functional polarization elements in bulk of dielectrics with controlled optical and structural properties.

Keywords: Fused silica, 3D micro-optical elements, filamentation, ultrashort laser pulses, wave plate.

DOI: 10.61011/EOS.2026.02.63468.8687-25

Introduction

Modern technologies of direct laser writing (DLW) with ultrashort pulses made it possible to achieve an unprecedented level of control over the formation of three-dimensional optical structures in transparent dielectrics. Due to the high peak power of femtosecond laser pulses, energy can be localized in a small volume of the material with nanometer precision, while the energy deposition time is significantly shorter than the characteristic times of thermal diffusion and electron-phonon relaxation. This provides for minimal thermal damage to the surrounding material and allows to implement high-quality modification even in materials with a wide transparency window, such as fused silica, sapphire, diamond, polymer dielectrics, etc. [1–3]. Multiphoton ionization initiated by intense radiation within the focal volume maintains efficient energy transfer to the crystalline or amorphous lattice without significant optical losses, which makes DLW a particularly appealing technology to develop elements of photonic integrated circuits, optical memory, and functional microstructures that control various properties of light: amplitude, phase, polarization, and spectral composition [4–6].

A special place among transparent dielectrics is held by fused silica, a material that combines high thermal and radiation resistance with a wide transparency range ($0.3-2.0\,\mu$m). When femtosecond laser pulses are focused, various types of micromodifications can be formed in its bulk: isotropic refractive index change (Type I), birefringent subwavelength gratings and nanopores (Type II/X), as well as microcavities (Type III) [7–11]. The physical mechanisms underlying the formation of such nanostructures are still the subject of active research. The most discussed models include the interference of the incident laser field with the plasma wave, local enhancement of the electromagnetic field, self-trapping of radiation, and interference of exciton-polaritons [12–17]. These processes lead to structural rearrangement of the material and the formation of defect centers, such as oxygen-deficient centers (ODC) and nonbridging oxygen hole centers (NBOHC), which determine both the optical and spectral properties of the modified regions [18].

Control of laser radiation parameters — wavelength, pulse duration, polarization and energy — makes it possible to finely tune the morphology of the nanostructure, optical anisotropy and transparency of the recorded regions of micromodification. It opens the opportunities for the development of three-dimensional arrays of nanogratings with the specified functional characteristics, including wave plates, polarization elements, color microfilters and nonlinearly optical metasurfaces [19–25].

In this paper the method of direct laser writing in bulk of fused silica formed a compact ($3 \times 3 \times 0.5$ mm) optical element that operates as a quarter-wave phase plate at wavelength of 633 nm. Birefringence caused by induced optical anisotropy provides for the required phase incursion

between the orthogonal polarization components. The complex study of spectral and polarization characteristics of the element was conducted in the range of 200−1000 nm, and spectral losses were analyzed in the ultraviolet (UV) and visible range related to light scattering in structural defects. It is demonstrated that in process of laser modification the fused silica crystal lattice is rearranged with a local gap of Si−O−Si-bonds and generation of ODC- and NBOHC-defects.

Experimental part

A microstructured optical element in bulk of fused silica was formed by DLW method using a femtosecond fiber ytterbium laser system Satsuma (Amplitude Systémes). The laser generated pulses with duration of 300 fs at the maximum energy per pulse up to 10 μJ and controlled repetition rate in the range of 1 Hz−500 kHz. The samples were plates made of synthetic fused silica (Suprasil 300, Heraeus) with thickness of 2 mm.

Laser radiation was focused into bulk of the sample for the depth of 730 μm using a microscope objective (LOMO) with a numerical aperture $NA = 0.1$. The estimated radius of the focal spot (by level $1/e^2$ of intensity) was $3.3 \pm 0.4\,\mu$m. The sample was moved relative to the focused beam of the recording femtosecond laser radiation using a precision two-axis stage H1P4A (Prior Scientific). The used positioner provides for accurate positioning not below $\pm 0.5\,\mu$m with the movement reproducibility not below $\pm 0.2\,\mu$m. The scanning speed was specified in software and was 500 μm/s. The speed stability in the range from 10 μm/s to several mm/s was within $\pm 1\%$ of the specified value. The structure was written as one layer at pulse energy of 2 μJ, repetition rate of 500 kHz. The structure was an array of 500 parallel lines with length of 3 mm and period of 6 μm. At the specified scanning and focusing parameters, an average of $N = 1.3 \cdot 10^4$ pulses hit each focal point, and the overlap of adjacent pulses perpendicular to the scanning direction (axis Y) was about 10%.

The optical properties of the written element were studied using a polarized-light microscope Zeiss Axioskop 40 (Carl Zeiss AG). Spectral characteristics of sample transmittance and absorption in the range of 200−1100 nm were registered in a double monochromator SF-2000 (OKB Spektr). For three-dimensional visualization of modified areas and analysis of luminescent properties, a confocal laser scanning microscope Confotec MR520 (Sol Instruments) was used. Luminescence was excited at wavelengths of 405 nm and 532 nm; the signal was collected through a Nikon microscope objective with a numerical aperture of $NA = 0.3$ and magnification of $10^{\times}$. The value of the optical path difference due to the birefringence of the written microstructure was measured using a compensation polarimeter LCC7201 (Thorlabs) when illuminating the element with a linearly polarized helium-neon laser ($\lambda = 633$ nm). The period of the written structure was determined by the position of the diffraction maxima arising when continuous radiation from a semiconductor laser (Cobolt 06-MLD, HÜBNER Photonics; $\lambda = 660$ nm, power 100 mW) passed through the sample. The angular position of the diffraction maxima was recorded using a CCD camera and used to calculate the structure period based on the diffraction grating equation.

Results and discussion

Optical properties

Fig. 1, *a* shows an optical image of a microoptic element formed in the fused silica bulk by DLW method. Macroscopically, the structure appears homogeneous and contains no visible cracks or damages; however, slight waviness is observed at the edges, due to the accumulated positioning error of the scanning system in process of writing. When observed under crossed polarizers (Fig. 1,*b*), inhomogeneous birefringence appears in the modified region, indicating the presence of an anisotropic internal structure. At higher magnification (Fig. 1, *c,d*), it becomes clearly visible that the micromodification region consists of parallel lines with a period of about 6 μm. High-resolution microscopy (Fig. 1, *d*) reveals the presence of microcavities uniformly distributed over the entire written region. Such cavities arise at high laser energy density and indicate local evaporation or rarefaction of the material in the focal region.

For a quantitative assessment of the structure periodicity, its diffraction properties were studied. Continuous laser radiation ($\lambda = 660$ nm, power 100 mW, beam diameter 2 mm) was transmitted through the sample, and the diffraction pattern was recorded on a screen. The deflection angle of the first diffraction maximum relative to the normal line to the surface allowed calculating the structure period using the diffraction grating formula $d = n\lambda / \sin\theta$. The obtained period value was $T = 6.0 \pm 0.3\,\mu$m, which is consistent with the diameter of the focused laser radiation spot. However, the diffraction efficiency in the first order turned out to be low — less than 4%. This indicates that the formed structure cannot be effectively used as a classical diffraction grating, which is likely due to partial damage of the micromodification region and the presence of microcavities that disrupt the regularity of the phase profile.

Despite the presence of the microstructure causing additional scattering, the optical element demonstrates rather high transmittance in the visible and near IR range: 60−80% in the interval of wavelengths 600−1100 nm (Fig. 1, *e*). As the wavelength decreases below 600 nm, drastic incidence of the transmittance is observed, which reaches practically zero values in deep ultraviolet light (200−300 nm). This behavior is typical for fused silica subjected to intense femtosecond laser irradiation and can be explained by the formation of oxygen defect centers — primarily ODC and NBOHC, which have intense absorption bands in the UV region [21]. Indeed, the absorption

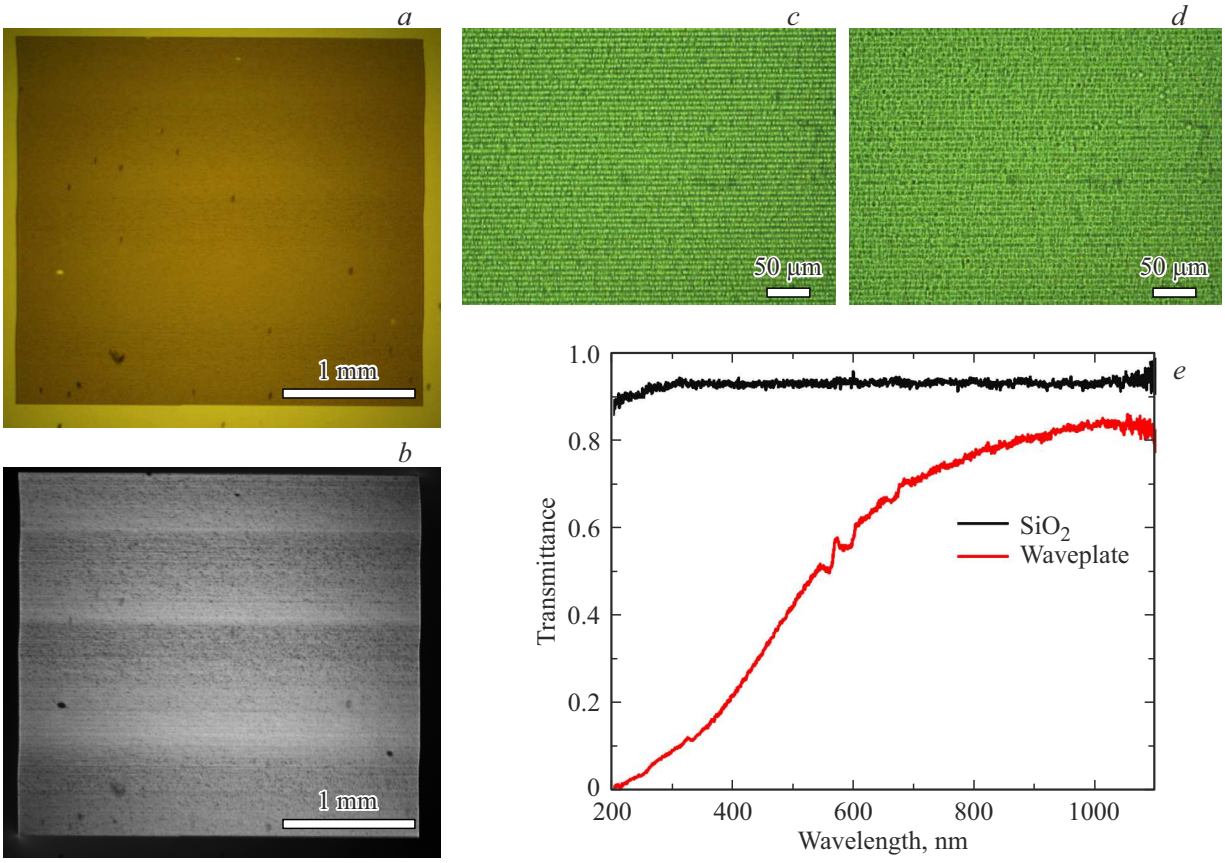

Figure 1. Images and transmittance spectra of the optical element in the fused silica bulk. (*a*) Lens with magnification $5^{\times}$, lighting at the bottom, without polarizers; (*b*) lens with magnification $5^{\times}$, lighting at the bottom, crossed polarizers; (*c*) lens with magnification $40^{\times}$, lighting at the bottom, without polarizers, depth 600 μm; (*d*) lens with magnification $40^{\times}$, lighting at the bottom, without polarizers, depth 550 μm; (*e*) spectra of transmittance of the optical element compared to a non-modified fused silica.

spectrum of oxygen-deficient centers (ODC) has the most intense bands in the deep ultraviolet light (maxima at $\sim 160-180$ nm and a weak broad band near 240–250 nm), while non-bridging oxygen hole centers (NBOHC) exhibit a characteristic absorption band in the visible region (~ 620 nm). The transmittance spectrum of the modified silica demonstrates a monotonic decrease in transmittance at $\lambda < 600$ nm (Fig. 1, *e*), which is most likely due to light scattering in inhomogeneities arising during DLW. Absorption at wavelengths corresponding to electronic transitions in oxygen-deficient centers may contribute additional losses near the bands ~ 250 nm (ODC) and ~ 620 nm (NBOHC). However, the spectral dependence of transmittance does not show pronounced anomalies characteristic of selective absorption in the indicated ODC and NBOHC bands, meaning a minor contribution of absorption compared to scattering in the studied spectral range.

The presence of high transmittance losses at $\lambda < 600$ nm limits the applicability of the element in the short-wavelength range. At the same time, it is known that thermal annealing at temperatures of $\sim 900^{\circ}$C can partially restore the silica structure, reducing the concentration of defects and, consequently, the level of scattering and absorption. However, such annealing also results in the lower value of induced birefringence, which is critical for the functionality of phase elements [21]. In this paper no thermal treatment was applied to maintain the maximum anisotropy required for operation of the element as a quarter-wave plate. Therefore, the formed structure is a compromise between the optical homogeneity, efficiency of birefringence and spectral losses caused by scattering and laser-induced defects. Further optimization of writing parameters (in particular, pulse energies and scanning speed) may allow decreasing the degree of material damage and accordingly the value of light scattering from heterogeneity and improving both transmittance and functional efficiency of the element.

Spectral measurements

To identify laser-induced structural and defect changes in fused silica, spectroscopic studies of Raman scattering (RS) and photoluminescence (PL) with cw laser excitation were carried out (Fig. 2).

Under pumping at a wavelength of 405 nm, the PL spectrum in the modified region is characterized by a

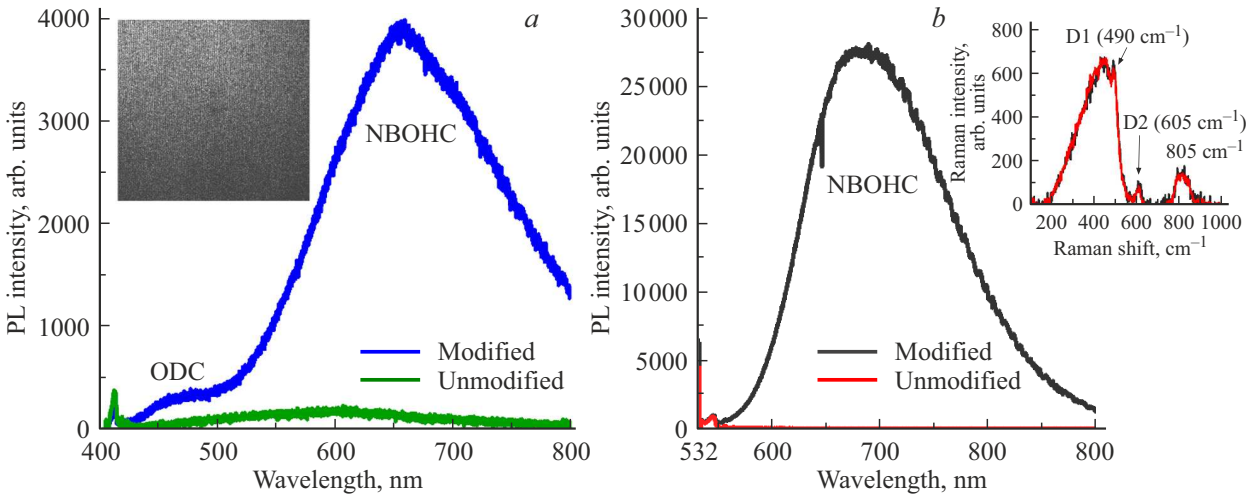

Figure 2. PL of oxygen defects ODC and NBOHC in fused silica when pumped with continuous laser radiation with wavelengths of 405 (a) and 532 nm (b). The inserts show a luminescent map with size of 1×1 mm for the micromodification region in the quarter-wave plate (Fig. 2, a) and the spectrum of combination scattering in the range of $0-1000\,\text{cm}^{-1}$ (Fig. 2, b).

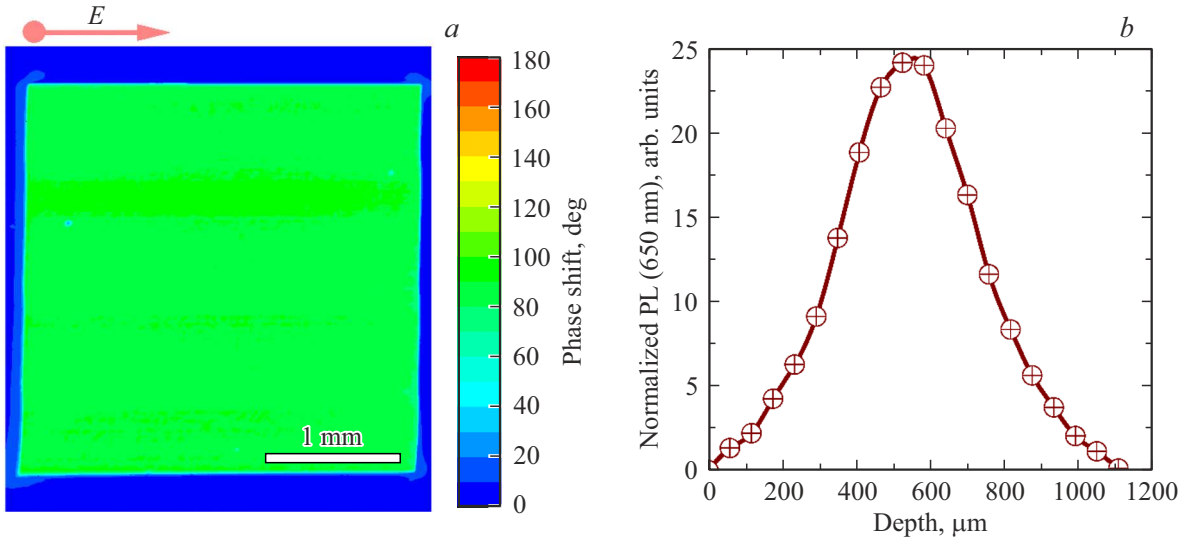

Figure 3. Pseudocolor map showing the distribution of the phase shift when radiation with a wavelength of 633 nm passes through a quarter-wave plate recorded in bulk of fused silica (a); PL depth profile of NBOHC-centers ($\lambda = 650$ nm) upon excitation at wavelength of 532 nm (b).

pronounced increase in intensity in two bands with maxima at 450 and 650 nm (Fig. 2, a). These bands are traditionally associated with radiation defects in silica: the short-wavelength component ~ 450 nm) is related to ODC, and the long-wavelength one (~ 650 nm) — to NBOHC [20]. To assess the spatial distribution of NBOHC-defects, a luminescence map of size 1×1 mm was obtained in fast confocal scanning mode based on the emission intensity at a wavelength of 650 nm. The map (insert in Fig. 2, a) demonstrates high signal uniformity, indicating a uniform distribution of NBOHC over the entire written region, including the boundaries between the bright and dark bands observed in crossed polarizers (Fig. 1, b). Under excitation at a wavelength of 532 nm, the luminescence of NBOHC-centers becomes dominant and exceeds the background signal from unmodified silica by more than two orders of magnitude (Fig. 2, b). This confirms the high concentration of these defects in the irradiated zone and indicates their key role in the formation of the optical properties of the structure.

Analysis of RS spectra in the range of $0-1000\,\text{cm}^{-1}$ (insert in Fig. 2, b) was carried out after subtracting the contribution of luminescence and normalization at the background signal intensity. The spectrum of fused silica demonstrates characteristic bands: wide R-band with maximum of about $440\,\text{cm}^{-1}$ caused by bending vibrations of bonds Si–O–Si, peaks D_1 ($490\,\text{cm}^{-1}$) and D_2 ($605\,\text{cm}^{-1}$) related to symmetric vibrations of three- and four-membered

rings SiO_4, and also a band at $\sim 805\,cm^{-1}$, corresponding to local deformations (stretching and bending) of bridging Si−O−Si-bonds [26]. After laser modification of intensity of D_1, D_2 and $805\,cm^{-1}$ bands normalized by R-band demonstrate minor, but reproducible increase. This indicates a partial damage to the medium-range order in the amorphous matrix of silica and local change of SiO_4-tetrahedron geometry.

Taken together, the RS and PL spectroscopy data indicate that the main structural transformations during femtosecond laser writing are associated with the breaking of bridging Si−O−Si-bonds and the subsequent formation of point defects — ODC and NBOHC. These are the defects that determine both the spectral losses in the UV region and the manifestation of birefringence due to the formation of an anisotropic nanostructure. The absence of significant changes in the R-band indicates the preservation of the overall amorphous silica matrix, while the enhancement of the D-bands reflects a local rearrangement of the network ring structure.

Birefringence

For a quantitative assessment of the phase shift induced by laser writing, birefringence measurements were carried out using a compensation polarimeter LCC7201 (Thorlabs). Radiation from a helium-neon laser with a wavelength of $\lambda = 633\,nm$ was used as a probe. The measurement results (Fig. 3, *a*) demonstrate a uniform distribution of the phase shift over the entire area of the modified region: $\Delta\phi = 90^\circ \pm 10^\circ$). This value corresponds to a quarter-wave delay between orthogonal polarization components, which confirms the functionality of the formed structure as a phase plate. The observed birefringence is caused by the formation of an anisotropic modification, which, according to modern research [7–11,13,15,23], is a subwavelength grating of alternating nanobands with different densities. The orientation of the bands is perpendicular to the polarization direction of the writing laser radiation [13,15,23]. Such a structure possesses effective optical anisotropy: the refractive index along the nanobands parallel to the laser radiation polarization in process of writing differs from the refractive index in the orthogonal direction, which leads to the birefringence observed in this paper. Since of the defects of such type the refractive index is higher along the polarization direction, in the quarter-wave wafer formed in bulk of fused silica (Fig. 3, *a*) the axis with high refractive index (slow axis) matches the scanning direction (axis X).

To estimate the value of birefringence Δn_{633}, ratio $\Delta n_{633} = R/L$ was used, where $R = \lambda\Delta\varphi/(2\pi)$ — optical path difference, and L — effective thickness of the modified layer. Since direct optical detection L is complicated due to weak contrast in the nonmodified silica, the structure thickness was detected using the PL profile of NBOHC-centers ($\lambda = 650\,nm$) upon excitation at wavelength of 532 nm. PL intensity is proportionate to the concentration of defects and therefore reflects the spatial distribution of laser-induced modification along the optical axis.

As you can see from Fig. 3, *b*, the PL profile has a pronounced maximum at the depth of $z \approx 560 \pm 20\,\mu m$, and the full width at half maximum (FWHM) is $L = 420 \pm 20\,\mu m$. Substituting $\Delta\phi = \pi/2$ and $L = 420\,\mu m$ into the expression for Δn_{633}, we get $\Delta n_{633} \approx 3 \cdot 10^{-4}$.

This value matches the typical values of birefringence achieved in writing of nanogratings in silica using femtosecond laser pulses. Notably, the position of the PL maximum ($z \approx 560 \pm 20\,\mu m$) differs significantly from the specified focusing depth of $z_f = 730\,\mu m$. This shift is explained by nonlinear effect of self-focusing arising in high peak capacity of laser pulses. Pulse energy in writing was $E_0 = 2\,\mu J$, duration — 300 fs, which corresponds to peak capacity $P \approx 6.7\,MW$. For fused silica at wavelength of 1030 nm the critical capacity of self-focusing is assessed as $P_{cr} \approx 4.5\,MW$ [27], and for $P > P_{cr}$ the conditions arise to generate a nonlinear focus inside the material.

The position of the nonlinear focus z_{sf} may be assessed using the modified self-focusing model [28]:

$$z_{sf} = \frac{k(I_0)\omega^2/2}{\sqrt{P/P_c - 1} + 2z_f/\left(k(I_0)\omega_0^2\right)}, \qquad (1)$$

where $k(I_0) = 2\pi n(I_0)/\lambda$ — wave number depending on intensity, $n(I_0) = n_0 + n_2 I_0$ — nonlinear refractive index, ω_0 — radius of the beam in the focal plane, $I_0 = 4E_0\sqrt{\ln 2}/(\pi^{3/2}\omega_0^2\tau)$ — peak intensity, $z_f = 730\,\mu m$ — geometric depth of focusing. Substitution of experimental parameters in equation (1) yields $z_{sf} \approx 620\,\mu m$, which is in agreement with the position of PL maximum ($560 \pm 20\,\mu m$). Thus, the observed shift of the maximum modification zone is a direct consequence of nonlinear self-focusing of laser radiation in the dielectric. This result underscores the need to account for nonlinear optical effects when designing three-dimensional optical elements by direct laser writing, especially in the modes close to the material damage threshold.

Conclusion

Using the femtosecond laser writing method, a homogeneous volumetric birefringent structure with a refractive index difference of $\Delta n \approx 3 \cdot 10^{-4}$ was formed in a bulk of fused silica, operating as a quarter-wave phase plate at a wavelength of 633 nm. Transmission spectroscopy showed that cavities and inhomogeneities, the formation of which significantly increases light scattering losses in the UV-visible spectral range, play a key role in determining the efficiency of the element formed by the DLW method. In addition, PL and RS studies of the element show that the modification process is accompanied by the generation of ODC- and NBOHC-defects, which are indicators of structural changes in the silica lattice and local gap of Si−O−Si-bonds. Displacement of the area of maximum modification relative to geometric focal

plane ($z = 730\,\mu$m $\rightarrow z \approx 560 \pm 20\,\mu$m) is explained by nonlinear self-focusing, which is confirmed by quantitative assessment of the non-linear focus position. The results demonstrate the potential of direct laser writing to create bulk polarization elements with the condition of the accounting of nonlinear effects and optimization of radiation modes

Funding

The study has been performed under the state assignment № FSFN-2025-0009.

Conflict of interest

The authors declare that they have no conflict of interest.

References

[1] K. Sugioka, Y. Cheng. Appl. Phys. Rev., **1** (4), (2014). DOI: 10.1063/1.4904320
[2] S.M. Eaton, J.P. Hadden, V. Bharadwaj, J. Forneris, F. Picollo, F. Bosia, B. Sotillo, A.N. Giakoumaki, O. Jedrkiewicz, A. Chiappini, M. Ferrari, R. Osellame, P.E. Barclay, P. Olivero, R. Ramponi. Adv. Quantum Technol., **2** (5,6), 1900006 (2019). DOI: 10.1002/qute.201900006
[3] K.C. Phillips, H.H. Gandhi, E. Mazur, S.K. Sundaram. Adv. Opt. Photonics, **7** (4), 684 (2015). DOI: 10.1364/AOP.7.000684
[4] S.I. Stopkin, A.S. Lipatiev, Yu.V. Mikhailov, S.S. Fedotov, T.O. Lipateva, V.N. Sigaev. Glass Ceram., **82** (5), 177 (2025). DOI: 10.1007/s10717-025-00768-4
[5] N.N. Skryabin, S.A. Zhuravitskii, I.V. Dyakonov, S.S. Straupe, A.A. Kalinkin, S.P. Kulik. Phys. Rev. Appl., **22** (6), 064079 (2024). DOI: 10.1103/PhysRevApplied.22.064079
[6] R. Drevinskas, P.G. Kazansky. APL Photonics, **2** (6), 066104 (2017). DOI: 10.1063/1.4984066
[7] M. Watanabe, H. Sun, S. Joudkazis, T. Takahashi, S. Matsuo, Y. Suzuki, J. Nishii, H. Misawa. Jpn. J. Appl. Phys., **37** (12B), L1527 (1998). DOI: 10.1143/JJAP.37.L1527
[8] Y. Shimotsuma, K. Hirao, J. Qiu, P.G. Kazansky. Mod. Phys. Lett. B, **19** (5), 225 (2005). DOI: 10.1142/S0217984905008281
[9] K.M. Davis, K. Miura, N. Sugimoto, K. Hirao. Opt. Lett., **21** (21), 1729 (1996). DOI: 10.1364/OL.21.001729
[10] W. Yang, E. Bricchi, P.G. Kazansky, J. Bovatsek, A.Y. Arai. Opt. Express, **14** (21), 10117 (2006). DOI: 10.1364/OE.14.010117
[11] H. Wang, Y. Lei, L. Wang, M. Sakakura, Y. Yu, G. Shayeganrad, P.G. Kazansky. Laser Photonics Rev., **16** (4), 2100563 (2022). DOI: 10.1002/lpor.202100563
[12] R. Stoian. Appl. Phys. A, **126** (6), 438 (2020). DOI: 10.1007/s00339-020-03516-3
[13] N.M. Bulgakova, V.P. Zhukov, Y.P. Meshcheryakov. Appl. Phys. B, **113** (3), 437 (2013). DOI: 10.1007/s00340-013-5488-0
[14] S.I. Kudryashov, P.A. Danilov, A.E. Rupasov, M.P. Smayev, A.N. Kirichenko, N.A. Smirnov, A.A. Ionin, A.S. Zolot'ko, R.A. Zakoldaev. Appl. Surf. Sci., **568**, 150877 (2021). DOI: 10.1016/j.apsusc.2021.150877
[15] A. Rudenko, J.P. Colombier, T.E. Itina. Phys. Rev. B, **93** (7), 075427 (2016). DOI: 10.1103/PhysRevB.93.075427
[16] M. Beresna, M. Gecevičius, P.G. Kazansky, T. Taylor, A.V. Kavokin. Appl. Phys. Lett., **101** (5), 053120 (2012). DOI: 10.1063/1.4742899
[17] Y.S. Gulina, A.E. Rupasov, G.K. Krasin, N.I. Busleev, I.V. Gritsenko, A.V. Bogatskaya, S.I. Kudryashov. JETP Lett., **119** (9), 652 (2024). DOI: 10.1134/S0021364024601003.
[18] A.V. Bogatskaya, E.A. Volkova, A.M. Popov. Appl. Phys. A, **131** (1), 79 (2025). DOI: 10.1007/s00339-024-08192-1
[19] S.I. Kudryashov, A.E. Rupasov, M.S. Kosobokov, A.R. Akhmatkhanov, G.K. Krasin, P.A. Danilov, B.I. Lisjikh, A. Abramov, E.D. Greshnyakov, E.V. Kuzmin, M.S. Kovalev, V.Y. Shur. Nanomaterials, **12** (23), 4303 (2022). DOI: 10.3390/nano12234303
[20] K. Mishchik, C. D'Amico, P.K. Velpula, C. Mauclair, A. Boukenter, Y. Ouerdane, R. Stoian. J. Appl. Phys., **114** (13), 133502 (2013). DOI: 10.1063/1.4822313
[21] G. Shayeganrad, X. Chang, H. Wang, C. Deng, Y. Lei, P.G. Kazansky. Opt. Express, **30** (22), 41002 (2022). DOI: 10.1364/OE.473469
[22] S.I. Kudryashov, P.A. Danilov, A.E. Rupasov, M.P. Smayev, N.A. Smirnov, V.V. Kesaev, A.N. Putilin, M.S. Kovalev, R.A. Zakoldaev, S.A. Gonchukov. Laser Phys. Lett., **19** (6), 065602 (2022). DOI: 10.1088/1612-202X/ac6806
[23] Y. Shimotsuma, M. Sakakura, P.G. Kazansky, M. Beresna, J. Qiu, K. Miura, K. Hirao. Adv. Mater., **22** (36), 4039 (2010). DOI: 10.1002/adma.201000921
[24] M. Beresna, M. Gecevičius, P.G. Kazansky, T. Gertus. Appl. Phys. Lett., **98** (20), 201101 (2011). DOI: 10.1063/1.3590716
[25] R. Osellame, H.J.W.M. Hoekstra, G. Cerullo, M. Polinau. Laser Photon. Rev., **5** (3), 442 (2011). DOI: 10.1002/lpor.201000031
[26] N. Varkentina, M. Dussauze, A. Royon, M. Ramme, Y. Petit, L. Canioni. Opt. Mater. Express, **6** (1), 79 (2015). DOI: 10.1364/OME.6.000079
[27] N. Vermeulen, D. Espinosa, A. Ball, J. Ballato, P. Boucaud, G. Boudebs, C.L.A.V. Campos, P. Dragic, A.S.L. Gomes, M.J. Huttunen, N. Kinsey, R. Mildren, D. Neshev, L.A. Padilha, M. Pu, R. Secondo, E. Tokunaga, D. Turchinovich, J. Yan, K. Yvind, K. Dolgaleva, E.W. Van Stryland. J. Phys. Photon., **5** (3), 035001 (2023). DOI: 10.1088/2515-7647/ac9e2f
[28] Yu.S. Gulina, J. Zhu, A.V. Gorevoy, N.I. Dolzhenko, P.A. Danilov, E.N. Rimskaya, S.I. Kudryashov. JETP Lett., **122** (1), 32 (2025). DOI: 10.1134/S0021364025607055.

Translated by M.Verenikina